ChemComm

Accepted Manuscript

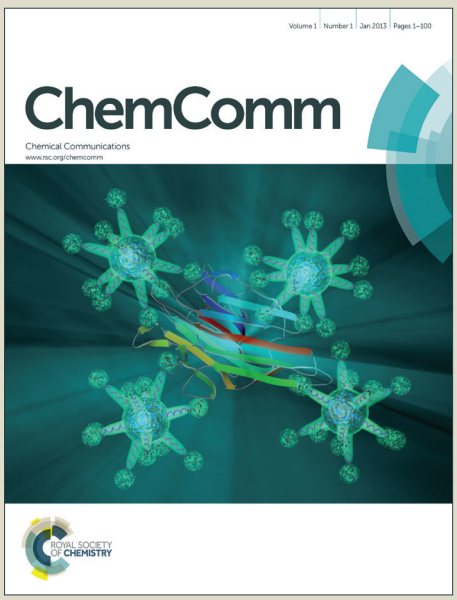

ROYAL SOCIETY OF CHEMISTRY

www.rsc.org/chemcomm

ChemComm

RSCPublishing

COMMUNICATION

Li-Se battery: absence of lithium polyselenides in carbonate based electrolyte

Cite this: DOI: 10.1039/xoxxoooooox

Yanjie Cui,[a] Ali Abouimrane,[a,*] Cheng-Jun Sun,[b] Yang Ren[b] and Khalil Amine[a]

Received ooth January 2012,
Accepted ooth January 2012

DOI: 10.1039/xoxxoooooox

www.rsc.org/

The lithiation mechanism of the Li-Se cell in a carbonate-based electrolyte is discussed. It is found that Se is directly reduced to Li_2Se in discharge without intermediate phases detected by in-situ X-ray diffraction or X-ray absorption spectroscopy. The reason is that the redox products Se and Li_2Se, as well as lithium polyselenides are insoluble in the electrolyte.

Worldwide research efforts are underway to develop an advanced energy storage system with high energy density, long cycle life, low cost, and safety. High energy density batteries are essential for all-electric vehicles or plug-in hybrid electric vehicles. At present, commercial batteries with typical capacities of 120–160 mAh g^{-1} are far below the much higher energy requirement of these applications.[1-3] Meeting this requirement will need breakthroughs in the area of novel electrode materials. Both Li/S and Li/O_2 batteries are attractive because they have the potential of providing 2 to 5 times the energy density of the lithium-ion batteries currently on the market, but these systems still face tremendous challenges.[1, 4-10] In addition, selenium, another group 16 element, was recently tested as a potential cathode material, which has a theoretical gravimetric capacity of 678 Ah kg^{-1} and theoretical volumetric capacity of 3268 Ah L^{-1}.[11] It is encouraging that a Se composite could be cycled versus both Li and Na at room temperature, as reported by Abouimrane et al. in 2012.[11] Then, in early 2013, Yang et al. successfully confined Se in the form of cyclic Se_8 molecules in ordered mesoporous carbon using a water-soluble binder and greatly improved the Li-Se battery performance.[12] Most recently, Luo et al. reported exceptional electrochemical performance of Se/mesoporous carbon composites in both Li- and Na-ion batteries: a reversible capacity of 480 mAh/g for 1000 cycles without any capacity loss for Li-ion batteries and an initial capacity of 485 mAh/g and 340 mAh/g retained after 380 cycles for Na-ion batteries.[13] In addition, Liu et al tested the electrochemical performance of nanoporous selenium and other Se/C composite as cathode materials of Li cells.[14, 15] These exciting results further supported the claim that the Li-Se battery is a promising energy storage system with high energy density. However, some fundamental problems remain to be resolved to further improve and optimize the performance of the Li-Se batteries.

In 2013, we reported the electrochemical reaction mechanism of the Li-Se battery in the ether-based electrolyte, namely, that Se is reduced to intermediates, polyselenides first then Li_2Se.[16] In addition, Luo et al. proposed that low-order polyselenide intermediates formed and were stabilized by mesoporous carbon, which avoided the shuttle reaction of polyselenides that occurs in the carbonate-based electrolyte.[13] While Yang et al. claimed that Se in the mesopores of CMK-3 directly transforms into Li_2Se, they attribute the single-plateau electrochemical behavior in the carbonate-based electrolyte to the mesoporous confinement effect.[12] Therefore, it is not clear whether there is polyselenide formation in a cycled Li-Se cell exhibiting a single plateau in the discharge process. Here, we present our recent results showing that even bulk Se cathode material exhibits a single plateau in the carbonate-based electrolyte in the voltage window of 0.8-3.5 V, and there are no polyselenides observed in the electrochemical process. This result clarifies the single-plateau mechanism of the Li-Se battery in carbonate-based electrolyte and is of great significance to further investigation and performance improvement of this promising electrode material.

Se-carbon composite cathodes[16] were cycled against Li metal anodes between 0.8 and 3.5 V in carbonate- and ether-based electrolyte. The former is designated GenII and consists of 1.2 M $LiPF_6$ dissolved in 3:7 volume ratio of ethylene carbonate (EC) and ethyl methyl carbonate (EMC); the latter is designated D2 and consists of 1M lithium bis(trifluoromethanesulphonyl)imide in 1:1 volume ratio of 1,3-dioxolane (DOL) and 1,2-dimethoxyethane (DME). The cell in D2 electrolyte was included for comparison. Figure 1a shows the voltage profiles of Li-Se cells cycled in both GenII and D2 electrolyte at a rate of 110 mA/g. As we reported earlier, for the cell

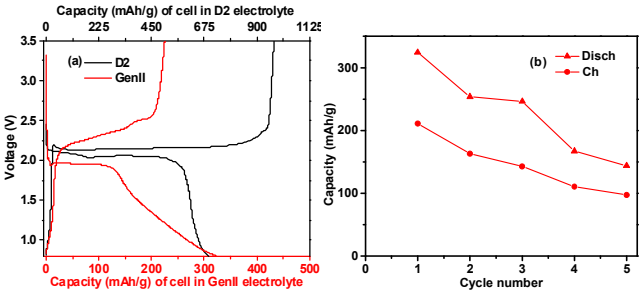

Fig. **1** Electrochemical performance of Li-Se cells: (a) voltage profiles of Li-Se cells in ether-based (D2) and carbonate-based (GenII) electrolyte and (b) cycling performance of Li-Se cell in GenII electrolyte.

with D2 electrolyte, there are plateaus at around 2.2 and 2.0 V in the first discharge, which correspond to the reduction of Se to high-order polyselenides Li_2Se_n($n\geq4$) and further reduction to Li_2Se_2 and Li_2Se. By contrast, in the cell with GenII electrolyte, we only observe one plateau, which is below 2 V. Further discharge and charge cycling showed that the capacity of the cell with the GenII electrolyte faded quickly, as shown in Fig. 1b. The mechanism underneath these phenomena is discussed below.

In-situ X-ray diffraction (XRD) and X-ray absorption spectroscopy (XAS) were applied to track the Se phase change, oxidation states, and phase distribution during electrochemical cycling. The in-situ XRD patterns and the cycling profile are shown in Figs. 2a and

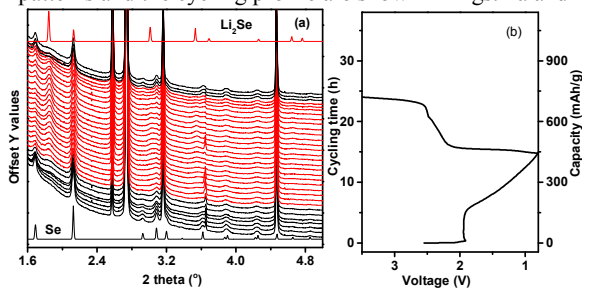

Fig. **2** In-situ high-energy XRD characterization of Li-Se cell in GenII electrolyte cycled between 0.8 and 3.5 V with a charging rate of 30 mA/g: (a) XRD pattern of the cell during cycling and the reference material Se and Li_2Se and (b) voltage profile.

2b, respectively. In Fig. 2a, the very strong peaks at 2θ = 2.74°, 3.16°, 4.47°, 2.57°, and 3.65° are due to the Al current collector and the Li anode. We focus here on the Se characteristic peaks at 1.69 and 2.13 ° and the Li_2Se peak at 1.85 ° to monitor the phase transition. With discharging, the intensity of the Se peak keeps decreasing; Li_2Se starts to appear at 1.86 V and keeps increasing to the end of discharge. The discharge capacity is 445 mAh/g at the charging rate of 30 mA/g. A small amount of Se remains by the end of discharge. By contrast, in the cell with D2 electrolyte, Se completely reduces into Li_2Se at the end of discharge, even at a charging rate of 110 mA/g, with capacity up to 680 mAh/g (Fig. 1a). In the GenII electrolyte, the capacity highly depends on the cycling rate: it is 320 mAh/g at a charging rate of 110 mA/g (Fig. 1a) and 445 mAh/g at a charging rate of 30 mA/g (Fig. 2b). This dependence suggests that the electrochemical reaction in the GenII electrolyte is a slow reaction. All these phenomena indicate a different discharge mechanism in different electrolyte. The XRD patterns proved that Se is partially reduced into Li_2Se by the end of discharge, and then Li_2Se is oxidized into Se at the end of charge without any intermediate phases formed during cycling.

Although XRD is a powerful technique in determining the crystalline phase change, it alone may not be conclusive in determining the phase change in a battery system, considering the complexity of a battery system including both solid and liquid phases. Therefore, we selected in-situ X-ray absorption near edge structure (XANES) spectroscopy to monitor the oxidation state changes during cell cycling, which can provide reliable information on all phases.[16, 17]

We carried out XANES measurements on a pouch cell made with GenII electrolyte and cycled at a rate of 110 mA/g. The selenium K-edge absorption, at 12,658 eV, arises from the transition of Se 1*s* core electrons to the unoccupied 4*p* states.[18] The Se K-edge of Li_2Se shifts to a higher energy (to12,660 eV). The abnormal shifts of the Li_2Se Se-edge toward higher energy could be explained by the reduced screening effect.[16] In addition, the S K-edge of Li_2S shifted to a higher energy, as reported by Gao et al. and Mori et al., due to the strong Coulombic interaction between the S^{2-} ion and the eight neighboring Li^+ ions, which reduces the screening effect.[19, 20]

A 2D contour plot of the Se XANES spectra recorded during the cell cycling is presented in Fig. 3a, with the voltage profile shown in Fig.

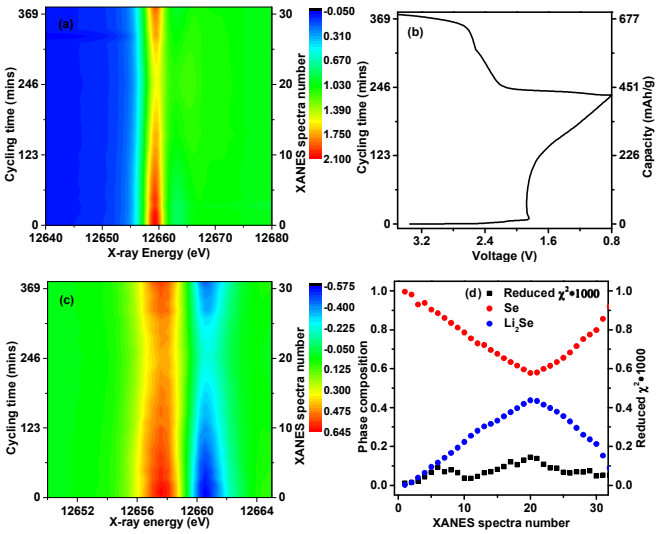

Fig. **3** In-situ XANES measurement for Li-Se pouch cell in GenII electrolyte: (a) normalized XANES spectra of the cycling cell, (b) voltage profile, (c) derivative of normalized XANES spectra, and (d) linear combination fitting of residue values and corresponding phase compositions in different state of charge/discharge.

3b. Generally, the energy position of the edge is determined as the lowest energy peak of the first derivative of the XANES spectra, as shown in Fig. 3c. Correlating Fig. 3c and 3b, we found that the edge positions did not undergo obvious shifts during the cell cycling even at the fully discharged state (0.8 V), in contrast to the significant energy shifts in the Li-Se cell with ether-based electrolyte.[16] However, the absorption of the Se-edge is weakened when the cell is discharged to 0.8 V.

Another common use of XANES is fingerprinting by linear combination fitting of XANES spectra of known species to determine the components in a mixture.[21] By selecting XANES spectra of the powder materials Se and Li_2Se as standards, we were able to determine the composition of the Se electrode at different states of charge/discharge by linear combination fitting of the XANES spectra measured during cell cycling with the Athena software package.[22] Most of the spectra are well fitted, illustrated by extremely small residues with reduced χ^2 from 0.012‰ to 0.144‰ as shown in Fig. 3d (black squares). These results are comparable to the values we obtained in multi-phase fitting with reduced χ^2 from 0.017‰ to 0.07‰ in the D2 electrolyte.[16] For Se and Li_2Se two-phase fitting, the spectra of cell with ether-based electrolyte leads to huge residues, with reduced χ^2 up to 5.676‰, indicating the formation of an intermediate phase. The fitting results in Fig. 3d suggest that there are no observable intermediate phases formed in the carbonate-based electrolyte cell, i.e., Se is directly transformed into Li_2Se and the reduction is not complete. This is consistent with the in-situ high-energy XRD analysis that Li_2Se formed in the discharge process, and Se reduction is not complete, as shown by the coexistence of Se and Li_2Se peaks. About 44% of Se is reduced into Li_2Se at the end of discharge, with a capacity of 425 mAh/g at a rate of 110 mA/g for a pouch cell. Most importantly, the in-situ XANES results confirmed that no lithium polyselenides formed in the electrochemical process.

To understand the lack of any intermediate phases with the carbonate-based electrolyte, we tested the solubility of Se in 3:7 volume ratio of EC/EMC solvent. We added 3.95 mg of Se and 4.64 mg of Li_2Se to 5 mL EC/EMC solvent (equivalent to 0.01 mol/L solution), respectively. Neither Se nor Li_2Se dissolved in the solvent,

as shown in Fig. 4. Then we took 1 mL solution from the Li_2Se-containing bottle and added it to the Se-containing bottle. No color

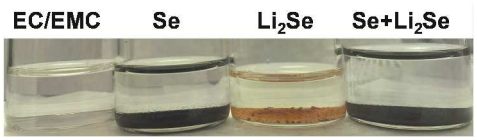

Fig. **4** Photograph of GenII electrolyte solvent EC/EMC alone, with insoluble Se, with Li_2Se, and with a combination of the two.

change was observed. By contrast, once Li_2Se dissolved ether-based solvent is added to the Se containing ether-based solvent, a dark-brown solution is observed, corresponding to Li_2Se_n ($n\geq4$) formation.[16] In addition, we tested the solubility of Li_2Se_n, it turns out that Li_2Se_n is insoluble in the carbonate based electrolyte (Fig. 1-2S, ESI). In the D2 electrolyte, the formation of soluble polyselenides facilitates lithium ion and electron transport, accelerating the electrochemical process; however, it also results in a shuttle effect. In the GenII electrolyte, Se is reduced into Li_2Se directly without the observation of Li_2Se_n phase since all those species are insoluble in the electrolyte. We further tested Se cathode prepared with water soluble binder sodium alginate (SA) for camparation with poly(vinylidene fluoride) (PVDF) binder (dissolved in N-methyl-2-pyrrolidone (NMP)), same voltage profiles were observed (Fig. 3S, ESI), except a slightly higher capacity for cathode with SA binder.[12] Therefore, we believe the solubility of the redox products in different electrolyte may actrually cause the differentlithiation mechanism.

The electrochemical reduction of Se (or Li_2Se oxidation) becomes difficult in a solid matrix than in the form of soluble species due to the poor lithium diffusion. Moreover, the weak connection between solid particles and carbon matrix being further broken down with repeated charge and discharge leads to worse interaction which leads to quick capacity drop and large polarization in the later cycles (Fig. 4S, ESI) in our case. However the feasibility of carbonate-based electrolyte in Li-Se cells has been proved by the work of Yang et al. and Luo et al., which demonstrated that the shuttle effect could be prevented by using carbonate based electrolyte and lithium ion and electron transport could be improved by Se confinement in the carbon matrix.[12, 13]

Conclusions

To summarize, in the Li-Se cell with carbonate-based electrolyte, the Se is directly reduced into Li_2Se, which leads to a single plateau during discharge. Due to the insolubility of Se, Li_2Se and lithium polyselenides in the EC/EMC electrolyte, no shuttle effect is expected. The key to further enhance the Li-Se battery performance will be on improving the lithium ion and electron transport property and intensifying the interaction between Se and conductive matrixes. This work demonstrated another advantage of the Li-Se cell over the Li-S cell: the absence of soluble polyselenides with the less expensive carbonate-based electrolyte avoids the need to prevent the shuttle effect.

Work done at Argonne National Laboratory(ANL) and use of the Advanced Photon Source and the Center for Nanoscale Materials were supported by the U. S. Department of Energy (DOE), Office of Science, Office of Basic Energy Sciences, under Contract No. DE-AC02-06CH11357. The pouch cells were produced at the U.S. DOE Cell Fabrication Facility (CFF), Argonne National Laboratory. The CFF is fully supported by the DOE Vehicle Technologies Program within the core funding of the Applied Battery Research for Transportation Program.

Notes and references

[a] Chemical Sciences and Engineering Division, Argonne National Laboratory, Argonne, Illinois, USA. * Email: abouimrane@anl.gov
[b] X-ray Science Division, Advanced Photon Source, Argonne National Laboratory, Argonne, Illinois, USA.

† Electronic supplementary information(ESI) available: Experimental details, lithium polyselenides solubility test, voltage profiles.

1. M. M. Thackeray, C. Wolverton and E. D. Isaacs, *Energy & Environ. Sci.*, 2012, **5**, 7854-7863.
2. J. M. Tarascon and M. Armand, *Nature*, 2001, **414**, 359-367.
3. M. S. Whittingham, *Chem. Rev.*, 2004, **104**, 4271-4301.
4. X. Ji and L. F. Nazar, *J. Mater. Chem.*, 2010, **20**, 9821-9826.
5. B. Zhang, X. Qin, G. R. Li and X. P. Gao, *Energy & Environ. Sci.*, 2010, **3**, 1531-1537.
6. T. Ogasawara, A. Debart, M. Holzapfel, P. Novak and P. G. Bruce, *J. Am. Chem. Soc.*, 2006, **128**, 1390-1393.
7. Z. Peng, S. A. Freunberger, Y. Chen and P. G. Bruce, *Science*, 2012, **337**, 563-566.
8. S. A. Freunberger, Y. Chen, Z. Peng, J. M. Griffin, L. J. Hardwick, F. Barde, P. Novak and P. G. Bruce, *J. Am. Chem. Soc.*, 2011, **133**, 8040-8047.
9. J.-T. Yeon, J.-Y. Jang, J.-G. Han, J. Cho, K. T. Lee and N.-S. Choi, *J. Electrochem. Soc.*, 2012, **159**, A1308-A1314.
10. F. Mizuno, S. Nakanishi, Y. Kotani, S. Yokoishi and H. Iba, *Electrochemistry*, 2010, **78**, 403-405.
11. A. Abouimrane, D. Dambournet, K. W. Chapman, P. J. Chupas, W. Weng and K. Amine, *J. Am. Chem. Soc.* , 2012, **134**, 4505-4508.
12. C.-P. Yang, S. Xin, Y.-X. Yin, H. Ye, J. Zhang and Y.-G. Guo, *Angew. Chem. Int. Ed.*, 2013, **52**, 8363-8367.
13. C. Luo, Y. Xu, Y. Zhu, Y. Liu, S. Zheng, Y. Liu, A. Langrock and C. Wang, *ACS Nano*, 2013, **7**, 8003-8010.
14. L. Liu, Y. Hou, X. Wu, S. Xiao, Z. Chang, Y. Yang and Y. Wu, *Chemical Communications*, 2013, **49**, 11515-11517.
15. L. Liu, Y. Hou, Y. Yang, M. Li, X. Wang and Y. Wu, *RSC Advances*, 2014, **4**, 9086-9091.
16. Y. Cui, A. Abouimrane, J. Lu, T. Bolin, Y. Ren, W. Weng, C. Sun, V. A. Maroni, S. M. Heald and K. Amine, *J. Am. Chem. Soc.*, 2013, **135**, 8047-8056.
17. D. C. Koningsberger and R. Prins, *X-ray Absorption: Principles, Applications, Techniques of EXAFS , SEXAFS and XANES*, John Wiley and Sons, New York, 1988.
18. S. C. B. Myneni, T. K. Tokunaga and G. E. Brown, *Science*, 1997, **278**, 1106-1109.
19. J. Gao, M. A. Lowe, Y. Kiya and H. D. Abruna, *J. Phys. Chem. C*, 2011, **115**, 25132-25137.
20. R. A. Mori, E. Paris, G. Giuli, S. G. Eeckhout, M. Kavcic, M. Zitnik, K. Bucar, L. G. M. Pettersson and P. Glatzel, *Anal.Chem.*, 2009, **81**, 6516-6525.
21. M. F. Lengke, B. Ravel, M. E. Fleet, G. Wanger, R. A. Gordon and G. Southam, *Environ. Sci. Technol.*, 2006, **40**, 6304-6309.
22. B. Ravel and M. Newville, *J. Synchrotron Radiat.*, 2005, **12**, 537-541.